ACS APPLIED MATERIALS & INTERFACES

www.acsami.org

Research Article

Anisotropic Photonic Microobjects with Dual Stopbands Formed from Single Photonic Dispersion and Their Application for Anticounterfeiting

Penghui Li, Yuandu Hu,* and Zhenzhong Yang*

Cite This: ACS Appl. Mater. Interfaces 2025, 17, 15969−15977

Read Online

ACCESS | Metrics & More | Article Recommendations | Supporting Information

ABSTRACT: Janus photonic microobjects have shown great potential in various fields due to their anisotropic shapes and tunable optical properties. Microfluidics is useful for constructing such photonic microobjects. The traditional method of injecting different colloidal photonic streams toward anisotropic multiple stopband photonic microobjects involves complicated and time-consuming procedures. Herein, an easy yet effective approach to fabricate Janus photonic microobjects with dual stopbands from a single stream of photonic components is proposed. A microfluidic device is used to prepare bullet-like, single-stopband photonic microobjects by virtue of the microchannel's confinement effect. Both the size and shape are readily regulated by adjusting the flow rate of the continuous phase. Under the protection of the desired region of the photonic microobjects with polystyrene (PS) film or silicone tube, the other region is selectively etched to generate a new photonic part. The Janus photonic microobjects with dual stopbands are achieved thereby. Precision control of the protection position of the single-stopband photonic microobjects provides the flexibility to achieve photonic microobjects with various segmental combinations. The porous structure at the etched region is conducive to further functionalization, for example, fluorescence performance, by filling polymers. The resultant photonic microobjects with strong information-encoding characteristics are promising in display and anticounterfeiting.

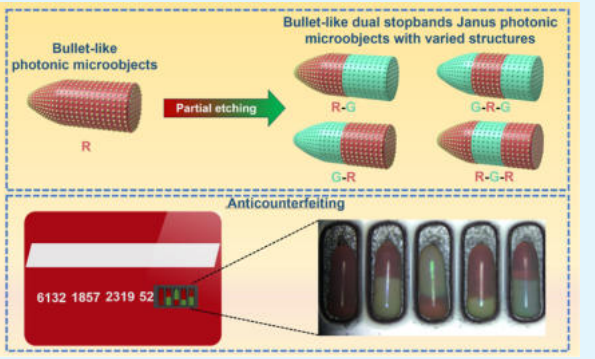

KEYWORDS: *Janus, photonic microobjects, dual-stopband, segmental combinations, anticounterfeiting*

1. INTRODUCTION

The emerging Janus photonic microobjects with anisotropic structures have received considerable attention in the past two decades.[1−4] The anisotropic structures render the microobjects additional functionalities, making the photonic microobjects attractive in various applications.[5−9] It is important to develop effective methods to construct microobjects with tunable composition and microstructure for the mounting demands of developing micro/nano devices. The anisotropic Janus photonic microobjects have been achieved by various methods, including lithography, etching, and controlled assembly. Among these methods, microfluidics is welcomed owing to the precision control of size, shape, and composition.[10−12] The photonic microobjects are capable of effectively manipulating light at microscale, demonstrating great potential applications in photonics, sensing, and imaging.[13] Zhao et al. prepared Janus structural color particles for ion detection using microfluidics and template methods.[14] Despite photonic microobjects with different functionalities being constructed by microfluidics in combination with other approaches,[15−19] it is highly required to integrate multiple stopbands within individual microobjects in a facile fashion. Anisotropic Janus photonic microobjects with an elongated shape have gained more attention.[20−22] The elongated geometry present in some microorganisms, such as paramecium, enables the microobjects new performance of propulsion and swimming.[23] Swager et al. have reported the ellipsoidal Janus photonic microobjects by the self-assembly of dendronized brush block copolymers inside a droplet. The photonic microobjects display orientation-dependent structural colors and anisotropic photonic properties.[21] Zhao and Gu et al. have utilized droplet microfluidics to fabricate photonic microobjects with a rod-like structure. The rod-like photonic microobjects with multiple stopbands are generated by the incorporation of multiple photonic components within the microobject.[22] Kim et al. prepared cylindrical and discoidal multicolor photonic microobjects using photolithography and flow lithography techniques, respectively.[24,25] These approaches either require the

Received: November 22, 2024
Revised: February 14, 2025
Accepted: February 18, 2025
Published: February 25, 2025

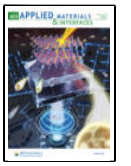

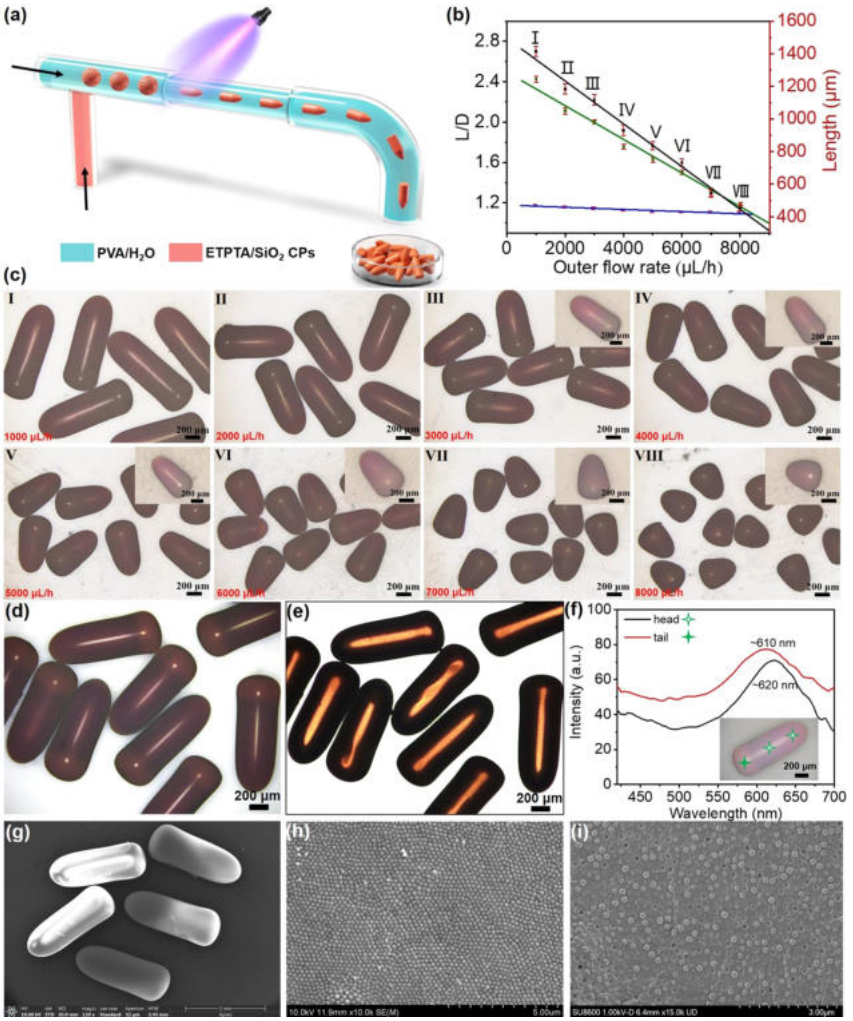

Figure 1. (a) Schematic fabrication of the bullet-like photonic microobjects by microfluidics. (b) Characteristic dimensions of the photonic microobjects depending on flow rate of the continuous phase. (c) Optical microscopy images of the bullet-like photonic microobjects prepared at different flow velocities of the continuous phase. Optical microscopy images of the red bullet-like photonic microobjects under reflection mode (d) and transmission mode (e). (f) Reflection spectra of the red bullet-like photonic microobjects. (g–i) SEM images of the red bullet-like photonic microobjects, surface, and the cross section.

preparation of photonic dispersions with different compositions or lack control over the size of the photonic microobjects. Among them, the discontinuous multistep process results in a low production efficiency for traditional photolithography. Although the flow lithography is a continuous process, it requires a low Reynolds number, a complex setup, and delicate control to integrate multiple stopbands into a single microobject. Therefore, there is an urgent need for an easy, yet effective method to fabricate Janus photonic microobjects. In the previous work, dual-stopband spherical photonic microobjects from a single photonic dispersion were prepared using droplet microfluidics combined with a partial etching process. However, the structural combination obtained was unitary.[26] Anisotropic photonic microobjects have the potential to obtain various structures, thus broadening the application range. Notably, this method does not involve the use of different colloidal photonic dispersions, thereby avoiding the preparation of colloidal particles with various sizes. This lowers the expenses while simultaneously increasing the experimental efficiency. Additionally, it is a very repeatable technique that enables fine-grained control over photonic microobject formation.

In this paper, we show the fabrication of bullet-like Janus photonic microobjects with dual stopbands from a single photonic composition, extending the method to manufacture photonic microobjects with anisotropic structure in terms of both their geometry and optical properties. Spherical droplets of photonic photocurable resin dispersion of monodispersed SiO_2 colloidal particles (CPs) were generated using a T-type microfluidic device. The droplets were subsequently delivered to a smaller tubing and transformed into a bullet-like shape for the UV-irradiated cross-linking, yielding bullet-like photonic microobject with a single stopband. Against this mother microobject, the bullet-like Janus microobject was created by integrating opal and inverse opal structures on an individual microobject. This was achieved by controllable etching of the desired region along the long axis while protecting the other region, for instance, etching the tail of the parent microobject while protecting the head. The resulting photonic microobjects can have both two and three segmental structures, increasing the structural combinations due to their nonspherical geometric structure. Preferential incorporation of functional materials within the inverse opal region endowed the microobject with new performances, such as fluorescence

https://doi.org/10.1021/acsami.4c20550
ACS Appl. Mater. Interfaces 2025, 17, 15969–15977

property. The Janus microobjects are promising in information encoding. Information encryption and anticounterfeiting were demonstrated by using the digital array of the Janus photonic microobjects as the substitution of the bank card numbers. This simple yet robust strategy to derive multiple functional Janus photonic microobjects paves the way in rational design and effective construction of miniaturized devices.

2. EXPERIMENTAL SECTION

2.1. Materials. Poly(vinyl alcohol) (PVA, M_w = 13k−23k, 87−89% hydrolyzed), ethoxylated trimethylolpropane triacrylate (ETPTA, ≥99%), *N*-isopropylacrylamide (NIPAAm, 97%), 2,2′-azobis(2-methylpropionitrile) (AIBN, 98%), deuterated DMSO (d^6-DMSO), *N*,*N*-dimethylformamide (DMF, anhydrous, 99.8%), lithium bromide (LiBr, >99%), and dichloromethane (CH_2Cl_2, ≥99.5%) were purchased from Sigma-Aldrich Co. Ltd. Ethanol (≥99.7%), aqueous ammonia (≥28%), tetraethyl orthosilicate (TEOS, electronic grade), polystyrene (PS, M_w ∼ 350k), and hydrofluoric acid (HF) were purchased from Aladdin Co. Ltd. 4-Vinyl-4′-methyl-2,2′-bipyridine (99%) was purchased from Ark Pharm, Inc. 2-Hydroxy-2-methyl propiophenone (photoinitiator 1173, >96.0%) was ordered from TiXi Ai HuaCheng Industry Development Co. Ltd. Ruthenium(4-vinyl-4′-methyl-2,2′-bipyridine)bis(2,2′-bipyridine) bis(hexafluorophosphate) [denoted as $Ru(bpy)_3$] was synthesized accordingly.[27] Dialysis membrane tubing (MWCO: 8k−14k Da) was provided by Fisher Scientific, Inc. All of the reagents were used as received.

2.2. Synthesis of SiO_2 CP. The SiO_2 CP of 170 nm was synthesized by the Stöber method.[28] Initially, 3 mL of deionized water, 8 mL of aqueous ammonia ($NH_3{\cdot}H_2O$), and 83 mL of ethanol were added to a conical flask. Then, 6 mL of TEOS was added and stirred at 60 °C at 500 rpm for the sol−gel process for 2 h. The product was centrifuged at 8000 rpm for 8 min and washed with ethanol. The purified SiO_2 CP was dispersed in ethanol for further use.

2.3. Preparation of ETPTA Suspension of SiO_2 CP. The dispersion of SiO_2 in ethanol was mixed with ETPTA resin (Figure S1a) containing 1% w/w photoinitiator 1173 at a certain volume fraction. Ethanol evaporated from the mixture at 70 °C to achieve the viscous suspension with a specific structural color. By changing the volume fraction of SiO_2, the color of the suspension was varied, as shown in Figure S1b.

2.4. Fabrication of Bullet-Like Photonic Microobjects. A T-type microfluidic device, as shown in Figure 1a, was used to prepare the bullet-like Janus photonic microobjects. An aqueous solution of 10% PVA and an ETPTA resin suspension of SiO_2 CP were used as the continuous and dispersed phases, with a tunable flow rate controlled by the corresponding injection pump (NE-1000, SyringePump). Two microfluidic channels were used with the corresponding diameters of inner/outer channels of 1.0 mm/1.5 mm and 0.58 mm/1.0 mm. At a certain flow rate of the dispersed phase through a narrow channel, the shape of the droplet changed from spherical to bullet-like due to the confinement effect. The bullet-like droplet was irradiated with a UV lamp (Gabon ZF-5, 16 W, Shanghai, China) to achieve the cured photonic microobject. By changing the flow rate of the continuous phase or the diameter of the channel, the size and shape of the bullet-like photonic microobject were greatly controlled.

2.5. Derivation of Dual-Stopband Janus Photonic Microobjects by Etching. The photonic microobject was placed vertically in a container (10 mm × 10 mm × 1.5 mm) covered with a polyimide double-sided tape. A desired amount of water was fed to partially immerse the photonic microobject arrays from the bottom and frozen at −20 °C. PS solution in CH_2Cl_2 (40 mg/mL) was fed to fill the container for the complete embedding from the top side of the arrays after evaporation of CH_2Cl_2. After the protected photonic microobject arrays were removed from liquid water, a 10% HF aqueous solution was carefully fed for etching the SiO_2 CP (Figure S2). The Janus photonic microobjects were separated and washed with water. After dissolution of the PS, the "green−red" (G-R) and "red−green" (R-G) dual-stopband Janus photonic microobjects were derived. In the case of an appropriate amount of PS solution, the middle part of the photonic microobject arrays was protected to derive a "green−red−green" (G-R-G) Janus photonic microobject after etching. The etching reaction was carried out at room temperature and normal laboratory conditions (24 °C, 40% RH). Typically, etching can be performed over a relatively large range (20−30 °C, 30−70% RH).

2.6. Synthesis of Ruthenium Polymer (pNIPAAm-*co*-Ru(bpy)$_3$). PNIPAAm-*co*-$Ru(bpy)_3$ copolymers were synthesized by free radical polymerization as shown in Figure S3. A 50 mL of ethanol/acetone solution (9:1 v/v) of NIPAAm (5.0 g) and ruthenium monomer (0.5 g) was dissolved in a 100-mL Schlenk flask with a magnetic stir bar. Then, 10 mL of ethanol solution containing 0.03 g of AIBN was added. After the solution was bubbled with N_2 for 30 min, polymerization was performed at 70 °C under N_2 for 6 h. The product was dialyzed against distilled water. ^{1}H NMR spectra and GPC traces of pNIPAAm-*co*-$Ru(bpy)_3$ are shown in Figure S4.

2.7. Preparation of Photonic Microobject Arrays. The dual-stopband Janus photonic microobjects were carefully aligned in the mold (Lianyungang Zhongre Optoelectronics Technology Co) (10 mm × 5 mm × 2 mm with grooves of 1.5 mm × 0.5 mm × 0.5 mm as shown in Figure S5) with tweezers according to the mathematical information represented. The card number on the front side was covered with the mold.

2.8. Characterizations. Transmission electron microscopy (TEM) images of SiO_2 CP were recorded on a TEM (JEOL, JEM-1400, Japan). The zeta potential of SiO_2 dispersions in water was measured by a Malvern Zetasizer Nano ZS90. An inverted optical microscope (LWD 300−38 LT, Beijing Cewei Optoelectronics, Beijing, China) was used to record the formation of droplets in the microfluidic device. An optical microscope (Olympus Corporation, Olympus BX53M, China) was used to record the bullet-like Janus photonic microobjects under different modes of reflection, transmission, and fluorescence. Reflection spectra of the photonic microobjects were recorded under an Olympus microscope (reflection mode) equipped with a fiber optic spectrometer (USB Flame-S, Ocean Insight, Inc., China). The fluorescence spectra of ruthenium-functionalized photonic microobjects were measured by a spectrofluorometer (Fluorat-02-Panorama, Celiss Inc., China) at an excitation wavelength of 420 nm. Morphologies of the bullet-like Janus photonic microobjects were characterized by a scanning electron microscope (SEM, Hitachi S-4800 and SU8600, Japan). Molecular weights of polymers were determined by gel permeation chromatography (GPC, Wyatt GPC/SEC-MALS system, Wyatt Technology Corporation, Santa Barbara, CA, USA) with 0.05 M LiBr DMF (HPLC grade) as the eluent. ^{1}H NMR spectra were recorded on the Bruker Avance III HD spectrometer using d^6-DMSO as the solvent.

https://doi.org/10.1021/acsami.4c20550
ACS Appl. Mater. Interfaces 2025, 17, 15969−15977

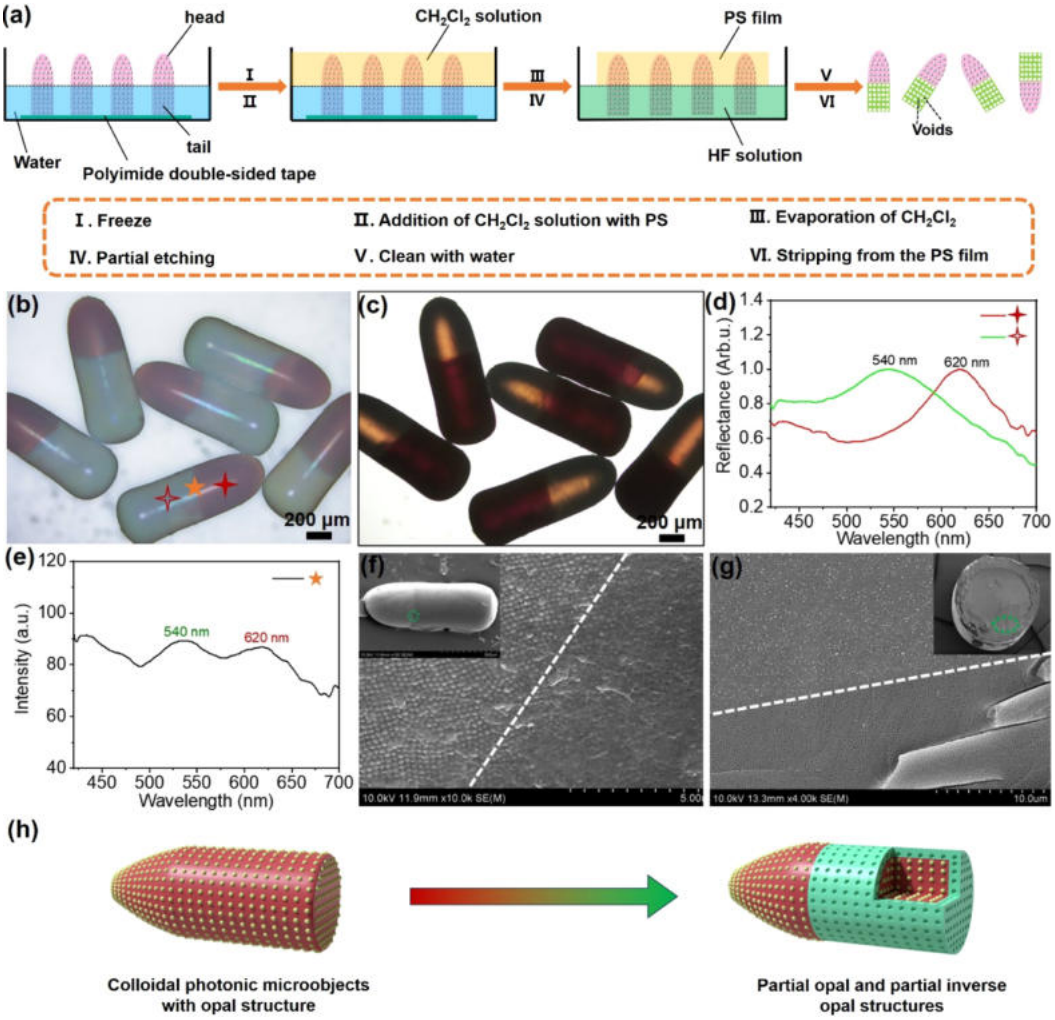

Figure 2. (a) Schematic fabrication of the bullet-like dual-stopband Janus photonic microobjects via protection-assisted etching. Optical microscopy images (b, reflection mode and c, transmission mode) of the photonic microobjects. (d–e) Reflection spectra of the photonic microobjects. SEM images of the surface (f) and cross-section (g) of the photonic microobjects. (h) Schematic structure of the bullet-like photonic microobject before and after etching.

3. RESULTS AND DISCUSSION

3.1. Preparation of Bullet-Like Photonic Microobjects. The bullet-like photonic microobjects were prepared using the T-type microfluidic device, as shown in Figure 1a. The ETPTA dispersion of SiO_2 CP and an aqueous solution of PVA were used as the dispersed and continuous phases. At a critical volume fraction of the SiO_2 CP, the interparticle repulsion is sufficient to form an ordered, non-close-packed face-centered cubic (FCC) lattice structure.[18] The system exhibits a bright structural color with characteristic reflection peaks under a photospectrometer. The bullet-like microobjects were solidified by the fast UV irradiation cross-linking. Currently, anisotropic colloidal microobjects with larger aspect ratios have been prepared through microfluidics. Zhao et al. prepared rod-like photonic microobjects based on the confinement of the collection capillary and relatively slow shearing.[29] In a similar microfluidic system, Zhao et al. found that when the flow rate of the dispersed phase remains constant, and as the flow rate of the continuous phase increases, the droplets take on a bullet-like.[30] In the aforementioned reports, droplets were collected directly in a confined channel. Differently, in our work, the dispersed phase was first sheared into monodisperse spherical droplets and then transported to a confined channel, which allows us to tune the droplet size in a facile fashion. The interplay between flow shearing and the confinement effect within the channel drives the morphological evolution of the droplets from spherical to bullet-like.[31] At a given flow velocity of a red photonic dispersed phase at 300 μL/h but varied velocity of the continuous phase, the size and shape of the bullet-like photonic microobjects were greatly tunable. The characteristic dimensions of length, width, and aspect ratio of the bullet-like photonic microobjects are shown in Figure 1b. The optical microscopy images of the bullet-like photonic microobjects prepared at different flow velocities of the continuous phase are shown in Figure 1c. The increment of the flow rate of the continuous phase gives rise to a more remarkable alteration in length than in width. The aspect ratio is decreased progressively. When the continuous phase flow rate was low (<0.8 mL/h), the dispersed phase formed a jet in the channel, resulting in uneven spherical droplets (Video S1). As the flow rate of the continuous phase increased, the dispersed phase was sheared at the intersection of the two phases, and the spherical droplets obtained had good monodispersity (Video S2 and Figure S6a–h). K is defined as the ratio of the spherical

https://doi.org/10.1021/acsami.4c20550
ACS Appl. Mater. Interfaces 2025, 17, 15969–15977

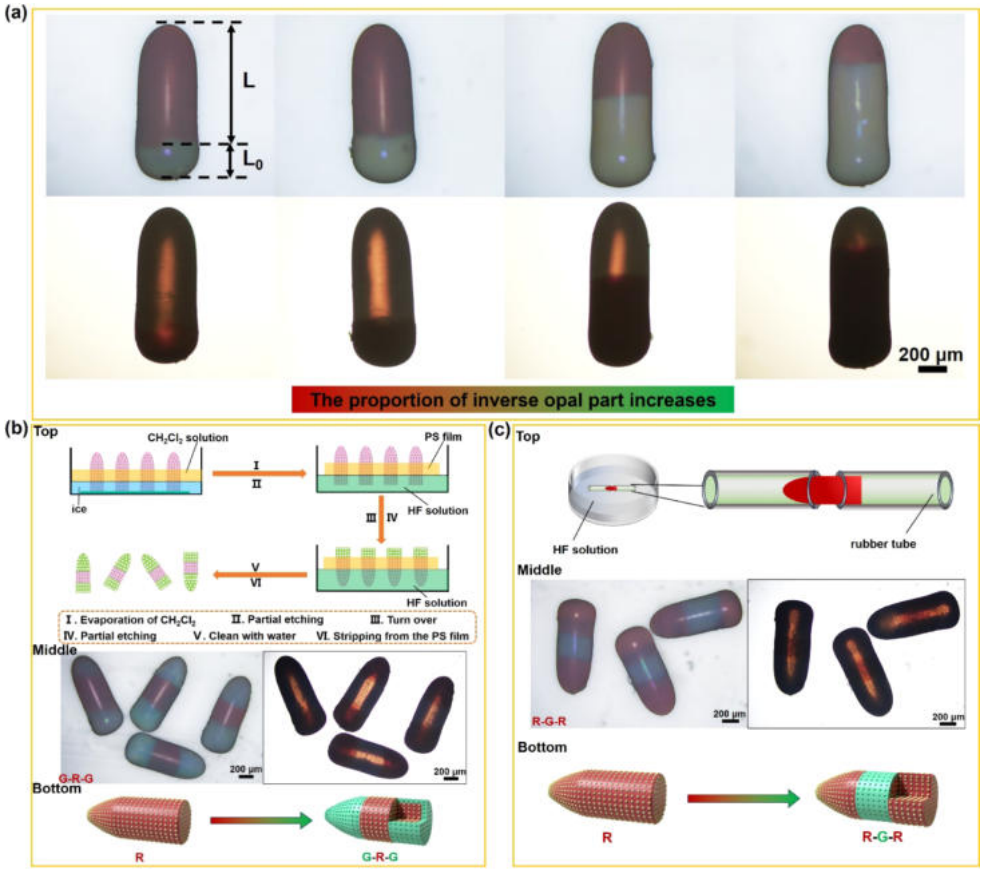

Figure 3. (a) Optical microscopy images (reflection mode and transmission mode) of the bullet-like dual-stopband Janus photonic microobjects of varied etching degrees. (b) Top: schematic preparation of the bullet-like dual-stopband Janus photonic microobject with a "green−red−green" structure. Middle: optical microscopy images (reflection mode and transmission mode) of the bullet-like Janus photonic microobject with a "green−red−green" structure. Bottom: schematic structure of the bullet-like photonic microobject before and after etching. (c) Top: schematic preparation of the bullet-like dual-stopband Janus photonic microobject with a "red−green−red" structure. Middle: optical microscopy images (reflection mode and transmission mode) of the bullet-like Janus photonic microobject with a "red−green−red" structure. Bottom: schematic structure of the bullet-like photonic microobject before and after etching.

droplet's diameter to the size of the confined channel (580 μm). When K was larger than ∼0.7, the spherical droplet deformed to bullet-like. When the continuous phase flow rate further increases (>10 mL/h), spherical droplets with a size much smaller than the diameter of the collection tube deformed to a heart shape, and K is below 0.7 (Figure S6i).

The photonic stopband could be readily regulated with the concentration and size of the SiO_2 CP. The SiO_2 CP of ∼170 nm (Figure S7) was selected to achieve the ETPTA resin suspension at two volume fractions of 21% and 32%. The corresponding red and green photonic microobjects were prepared by droplet microfluidics (Figures 1d, e and S8). The prepared red, bullet-like, photonic microobject was selected as the example. The reflection spectra of the red photonic microobject are shown in Figure 1f. In addition, it exhibits angle-independent photonic properties, and the spectra observed in different directions of the minor axis and major axis remain unchanged (Figure S9). The diameter ratio of two channels was fixed at 1:0.58, and the flow velocity ratio at the two regions was fixed at 1:3. The narrower channel leads to an increased flow velocity of the continuous phase; an abrupt deformation of the droplets should bring in the spacing change between the SiO_2 CPs in the bullet-like photonic microobjects. The spacing at the head region is slightly larger than that at the tail part. The reflection peak of the head is red-shifted compared to that of the tail part. The maximum wavelength (λ) of the reflected color was estimated by the Bragg equation for a normal-incident beam onto the (111) plane of an fcc structure:[18]

$$\lambda = 2dn_{\text{eff}} = \left(\frac{\pi}{3\sqrt{2}\phi}\right)^{1/3}\left(\frac{8}{3}\right)^{1/2} D(n_{\text{silica}}^2\phi + n_{\text{pETPTA}}^2(1-\phi))^{1/2} \quad (1)$$

where n_{eff} is the effective refractive index of the photonic microobject. D is the diameter of the SiO_2 CP. ϕ represents the volume fraction of the SiO_2 CP. n_{silica} and n_{pETPTA} are the refractive indices of the SiO_2 CP (1.45) and pETPTA matrix material (1.47).[18] D = 170 nm, ϕ = 0.23 or 0.32. The λ values were calculated at 602 and 539 nm, which were closely consistent with the experimental results. The SiO_2 CPs are orderly packed into a hexagonal array in the whole region of the photonic microobjects (Figure 1g−i).

3.2. Preparation of the Bullet-Like Dual-Stopband Photonic Microobjects. The integration of the dual-stopband structure by protective etching of the bullet-like photonic microobject was achieved as shown in Figure 2a. The as-prepared, bullet-like, photonic microobjects were adhered at the bottom sides onto a polyimide double-sided tape, ensuring

https://doi.org/10.1021/acsami.4c20550
ACS Appl. Mater. Interfaces 2025, 17, 15969−15977

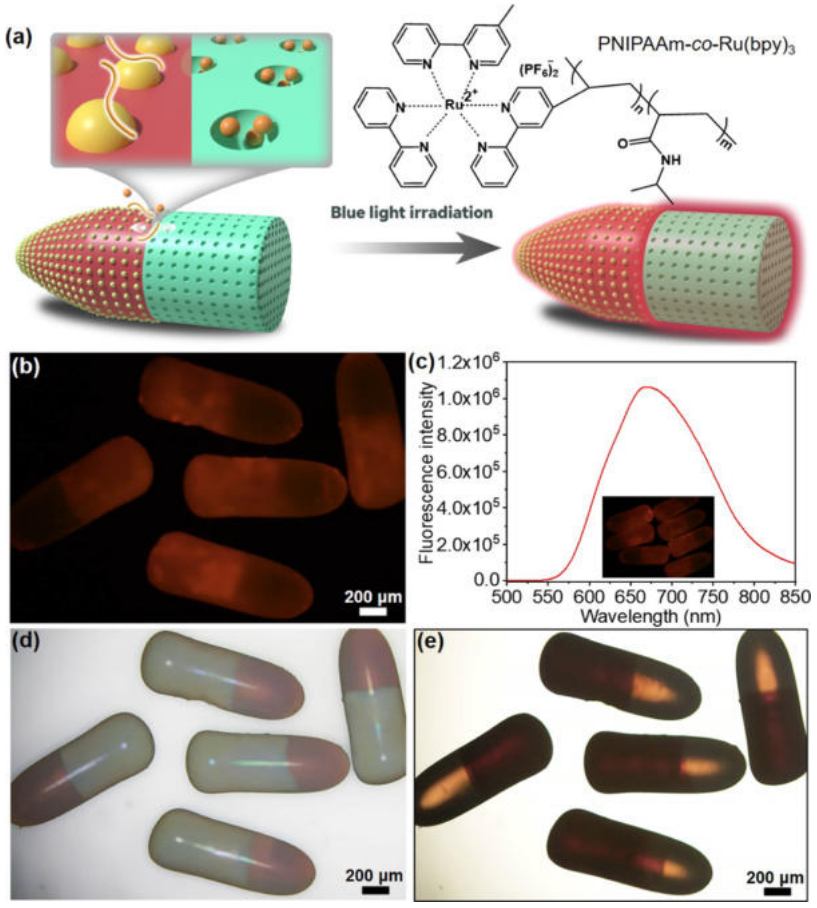

Figure 4. (a) Schematic filling of ruthenium-functionalized polymers at the bullet-like dual-stopband Janus photonic microobject. Fluorescence (b) and optical (d,e reflection and transmission modes) and microscopy images of the bullet-like dual-stopband Janus photonic microobject immersed in ruthenium polymer solution for 20 h. (c) Fluorescence spectra of the ruthenium-functionalized bullet-like Janus photonic microobject.

upward orientation. A certain amount of water was fed to partially immerse the arrayed microobjects, followed by solidification at −20 °C. A certain amount of PS solution in CH_2Cl_2 was fed to completely fill the array. After evaporation of CH_2Cl_2, the head part of the array was completely embedded and thus protected with the PS film. After elevating the temperature to melt the ice, the PS-protected array was removed and loaded in HF solution for the selective etching (more careful operation!). After SiO_2 CPs were etched, the inverse opal structure was generated on the surface at the tail part. This protection was not only effective on the surface but also effectively slowed the diffusion of HF into the interior of the protected area (Figure S10). Both opal and inverse opal structures were thus integrated at the bullet-like Janus photonic microobject (Figure S11a). The etching became slower from the initial rate of ∼1.78 to ∼0.23 μm/min with the etching depth (Figure S11b). At an early stage of the etching, the inverse opal structure coexists with the beneath opal structure at the tail part. In comparison with the close-packed SiO_2 CPs, the non-close-packed structure requires a longer time to achieve the desired etching degree. It is worth mentioning that the etching depth does not affect the optical properties of the photonic microobject (Figure S12). With further prolonging the etching time to 5 h, the etching was beyond control to influence the SiO_2 CPs at the protected region. As a result, the boundary between inverse opal and opal structures becomes less distinct (Figure S13).

The mother photonic microobject displays red under an optical microscope, and the derived dual-stopband Janus photonic microobject demonstrates red and green colors (reflection mode) at the two parts after 1 h of etching (Figure 2b). The corresponding golden yellow and deep red are shown in transmission mode (Figure 2c). After the removal of the SiO_2 CPs, the reflective peak shifts blue with the stopband broadening due to the increased refractive index mismatch. The reflection peak shifts from 620 to 540 nm with the etching (Figure 2d). The resultant photonic microobjects show two peaks at 540 and 620 nm (Figure 2e). This method is also applicable to smaller photonic microobjects (Figure S14). The structural color of the dual-stopband Janus photonic microobject is angle-independent and does not change with the viewing angle (Figure S15). Similarly, the initial green photonic microobject was converted into the heterogeneous microobject with two reflection peaks at 545 and 475 nm (Figure S16). After etching SiO_2 CPs at the tail part, macropores are present under SEM (Figure 2f,g). No macropores are found at the protected part. There exists a distinct boundary between the two regions. Figure 2h illustrates the transformation of the initial photonic microobject with a single stopband into dual stopbands.

3.3. Control of the Stopbands. The structural color originates from the selective reflection of visible light by periodically ordered structures with a dielectric contrast.[32,33] It is of great significance to fine-tune the structural colors of artificial photonic microobjects. In the current case, the

https://doi.org/10.1021/acsami.4c20550
ACS Appl. Mater. Interfaces 2025, 17, 15969−15977

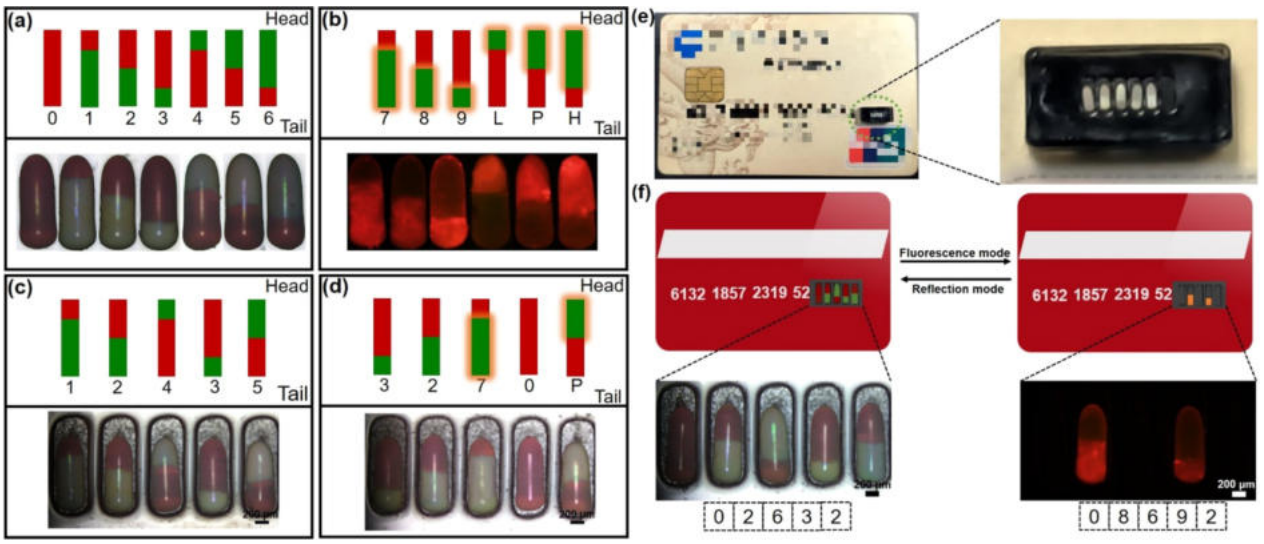

Figure 5. (a,b) Schematic figure, optical (reflection mode), and fluorescence microscopy images of the bullet-like Janus photonic microobjects with different encoded information. (c,d) Schematic figure and optical (reflection mode) microscopy images of the bullet-like Janus photonic microobjects array with encoded information. (e) Photograph of the five-digital number at the bank card after being covered and substituted by an array of the bullet-like Janus photonic microobjects. (f) Optical (reflection mode) and fluorescence microscopy images of the array encoding under the two modes.

stopband behavior of the bullet-like Janus photonic microobjects can be readily tuned by altering the protection and etching degrees. The degree of protection of the opal structure can be controlled by the amount of water used to immerse the tail part (Figure S18). A small amount of water leads to a small portion of the inverse opal structure in the dual-stopband Janus photonic microobject. The portion of inverse opal (L_0) is tunable, as shown in Figure 3a, achieving a series of bullet-like Janus photonic microobjects with a "red−green" (R-G) structure. Similarly, etching can be conducted at the head region of the bullet-like photonic microobject to generate the corresponding "green−red" (G-R) structure (Figure S19).

On the other hand, when the PS solution in CH_2Cl_2 was insufficient to cover the whole head region of the array, protection of the middle part of the bullet-like photonic microobjects was achieved. The opposite parts of the photonic microobjects were selectively etched, as shown in Figure 3b (top). The bullet-like Janus photonic microobject of the "green−red−green" (G-R-G) structure was achieved (Figure 3b [middle]). Figure 3b (bottom) illustrates the process of generating the G-R-G structure. Alternatively, while protecting both ends of the initial single stopband photonic microobject with rubber tubes (Figure 3c [top]), the corresponding "red−green−red" (R-G-R) structure was achieved by etching (Figure 3c [middle]). This process is illustrated in Figure 3c (bottom). Reflection spectra of the R-G-R and G-R-G structures are shown in Figure S20. Therefore, the simple controllable protection provides a convenient method to achieve a family of bullet-like Janus photonic microobjects with varied structures and thus stopband performances (Figure S21). For anisotropic bullet-like photonic microobjects, the orientation is indeed an important influencing factor. The microobjects need to be fixed with double-sided tape in the early stage, and it cannot be guaranteed that all the microobjects are in the same orientation. Undoubtedly, this is a simple and effective approach that paves the way for the design and building of other miniaturized devices. Therefore, how to better control the orientation of photonic microobjects and make selective etching methods widely applicable is under our consideration and further investigation.

3.4. Functionalization of the Photonic Microobjects.

Functionalization is achieved by filling the macropores in the inverse opal region with desired materials. As reported, the deposition of gold or aluminum in the photonic porous structure of the etched microsphere imparts plasmonic color and electrical responsiveness.[34] It is interesting to fill ruthenium-functionalized polymers within the inverse opal structure owing to their multifunctionalities of thermoresponsiveness, catalysis, and fluorescence performance.[35] After immersion of the dual-stopband microobject in an aqueous solution of the ruthenium-functionalized polymer, the microobject could be readily modified with fluorescence performance, as illustrated in Figure 4a. The inverse opal region is filled with the ruthenium-functionalized polymer, displaying a stronger fluorescence signal (Figure 4b). In addition, the negative charge of SiO_2 CPs can interact with and absorb the ruthenium-functionalized polymers via electrostatic interaction (Figures S22 and S23). The fluorescence spectra of bullet-like Janus photonic microobjects are shown in Figure 4c. The corresponding optical microscopy images are shown in Figure 4d,e. The structural color and reflection spectra of the photonic microobject are less influenced by filling the ruthenium polymer (Figures S24 and S25), implying that the two signals are orthogonal. This fact is important for information anticounterfeiting.

3.5. Information Coding and Anticounterfeiting.

Positions of the opal and inverse opal parts and the volume ratio in the Janus photonic microobjects are tunable, providing a huge potential in information encoding. The bullet-like Janus photonic microobjects with varied structures and fluorescence properties are shown in Figure 5a,b. A Janus photonic microobject with a protected-to-etched ratio of 1/2 was selected as the example. The structure was endowed by writing the information on "1" (Table S1). The bullet-like Janus photonic microobjects were arrayed in a mold according to the designed program. As shown in Figure 5c, the information was

https://doi.org/10.1021/acsami.4c20550
ACS Appl. Mater. Interfaces 2025, 17, 15969−15977

read as "12435" Precision acquisition of the information by structural color was further enhanced by fluorescence information. As shown in Figure 5d, the information on "32105" was read solely by the structural color. The exact information on "3270P" was read by combinational fluorescence information, as shown in Figure S26. Therefore, authentication was applied in the information encoding. Combinational information on "32105" from the reflection mode and "3270P" from the fluorescence mode determines a safety password. The hidden password could be exactly determined by the dual modes, implying a high level of information confidentiality.

Surfaces of different cards were applied for information encoding and anticounterfeiting by the Janus photonic microobjects. After covering a five-digit number on the bank card with a mold, the card number information was substituted by an ordered array of bullet-like Janus photonic microobjects, as shown in Figure 5e. Both optical images of the reflection mode (left) and fluorescence microscopy (right) of the array are shown in Figure 5f. The digital information could be read through the encoding, as shown in Table S1. The information on "02632" was read from the structural color under the reflection mode, while the hidden message of "08692" was encoded under the fluorescence mode. The combinational encoding reveals the exact information on "08692" on the bank card.

4. CONCLUSIONS

We have proposed a facile method to generate anisotropic Janus photonic microobjects with a dual stopband through a controllable etching process under protection. SiO_2 CPs/ETPTA composite bullet-like photonic microobjects with a single stopband were fabricated using a T-type microfluidic device. A subsequent controllable etching of the SiO_2 CPs under protection was conducted to achieve the inverse opal structure, rendering dual-stopband performance at bisegmental microobjects ("red−green" [R-G] or "green−red" [G-R]) or trisegmental microobjects ("green−red−green" [G-R-G] or "red−green−red" [R-G-R]). Ruthenium polymers were filled within the inverse opal region to render the dual-stopband Janus photonic microobjects fluorescence performance. The combination of the stopband behavior and fluorescence performance using the bullet-like Janus photonic microobject arrays makes information storage and encoding easier with fidelity. The Janus photonic microobjects are highly potential in digital display and anticounterfeiting. The strategy is generally to construct more complex photonic microobjects in huge data encoding and anticounterfeiting. The manufacturing of bullet-like dual-stopband Janus photonic microobjects has shown considerable benefits with this approach, but it can still be improved; future optimization efforts should focus on achieving flexible control of the orientation of anisotropic photonic microobjects, for example, by adding magnetic components, which would open the door to large-scale manufacturing.

■ ASSOCIATED CONTENT

Supporting Information

The Supporting Information is available free of charge at https://pubs.acs.org/doi/10.1021/acsami.4c20550.

TEM image and zeta potential of the SiO_2 CP; ^1H NMR spectrum and GPC trace of pNIPAAm-*co*-Ru(bpy); optical microscopy images of the bullet-like dual-stopband Janus photonic microobjects of varied etching degrees; optical microscopy images of the cross-section of the bullet-like photonic microobjects after different etching periods; optical microscopy images and reflection spectra of green bullet-like photonic microobjects before and after etching; reflection spectra of R-G-R and G-R-G bullet-like dual-stopband Janus photonic microobjects; fluorescence microscopy image of an array of the bullet-like Janus photonic microobjects; encoding by the bullet-like photonic microobjects (PDF)

Depiction of the dispersed phase formed a jet in the channel, resulting in uneven spherical droplets when the continuous phase flow rate is low (MP4)

Depiction of the dispersed phase sheared at the intersection of the two phases, and the spherical droplets obtained had good monodispersity, as the flow rate of the continuous phase increased (MP4)

■ AUTHOR INFORMATION

Corresponding Authors

Yuandu Hu − *Department of Materials Science and Engineering, School of Physics Science and Engineering, Beijing Jiaotong University, Beijing 100044, China; Guangdong Provincial Key Laboratory of Technique and Equipment for Macromolecular Advanced Manufacturing, South China University of Technology, Guangzhou 510641, China; State Key Laboratory of Molecular Engineering of Polymers (Fudan University), Shanghai 200438, China; Department of Chemical Engineering, Tsinghua University, Beijing 100084, China;* orcid.org/0000-0001-5510-2950; Email: huyd@bjtu.edu.cn

Zhenzhong Yang − *Department of Chemical Engineering, Tsinghua University, Beijing 100084, China;* orcid.org/0000-0002-4810-7371; Email: yangzhenzhong@tsinghua.edu.cn

Author

Penghui Li − *Department of Materials Science and Engineering, School of Physics Science and Engineering, Beijing Jiaotong University, Beijing 100044, China*

Complete contact information is available at: https://pubs.acs.org/10.1021/acsami.4c20550

Author Contributions

P.L. performed the experimental studies, analyzed the experimental data, and wrote the original manuscript. The manuscript was written through the contributions of all authors. All authors have given approval to the final version of the manuscript.

Notes

The authors declare no competing financial interest.

■ ACKNOWLEDGMENTS

This work is supported by the Fundamental Research Funds for the Central Universities (No. KVJBMC23001536 (Y. H.), No. 2024YJS195 (P. L.). Y. H. is grateful for the funds from the Guangdong Provincial Key Laboratory of Technique and Equipment for Macromolecular Advanced Manufacturing (No. 20240518), the State Key Laboratory of Molecular Engineering of Polymers (No. K2024-15), and the Key Laboratory of

Advanced Materials of the Ministry of Education (No. Advmat-2402). Thanks to eceshi (www.eceshi.com) for the ^{1}H NMR test.

REFERENCES

(1) Wang, H.; Liu, Y.; Chen, Z.; Sun, L.; Zhao, Y. Anisotropic Structural Color Particles from Colloidal Phase Separation. *Sci. Adv.* **2020**, *6* (2), No. eaay1438.
(2) Velev, O. D.; Lenhoff, A. M.; Kaler, E. W. A Class of Microstructured Particles through Colloidal Crystallization. *Science* **2000**, *287*, 2240−2243.
(3) Wang, H.; Zhang, H.; Chen, Z.; Zhao, Y.; Gu, Z.; Shang, L. Polymer-Based Responsive Structural Color Materials. *Prog. Mater. Sci.* **2023**, *135*, 101091.
(4) Wang, H.; Zhang, H.; Bian, F.; Zhang, D.; Gu, H.; Kong, B. Bioinspired Bioassay Platforms Derived from Colloidal Crystals with Topological Shapes. *Aggregate* **2024**, *5* (2), No. e467.
(5) Guo, Q.; Li, Y.; Liu, Q.; Li, Y.; Song, D. Janus Photonic Microspheres with Bridged Lamellar Structures via Droplet-Confined Block Copolymer Co-Assembly. *Angew. Chem. Int. Ed.* **2022**, *61* (5), No. e202113759.
(6) Goodling, A. E.; Nagelberg, S.; Kaehr, B.; Meredith, C. H.; Cheon, S. I.; Saunders, A. P.; Kolle, M.; Zarzar, L. D. Colouration by Total Internal Reflection and Interference at Microscale Concave Interfaces. *Nature* **2019**, *566*, 523−527.
(7) Wang, Z.; Li, R.; Zhang, Y.; Chan, C. L. C.; Haataja, J. S.; Yu, K.; Parker, R. M.; Vignolini, S. Tuning the Color of Photonic Glass Pigments by Thermal Annealing. *Adv. Mater.* **2023**, *35* (34), 2207923.
(8) Zhang, Z.; Raymond, J. E.; Lahann, J.; Pena-Francesch, A. Janus Swarm Metamaterials for Information Display, Memory, and Encryption. *Adv. Mater.* **2024**, *36* (45), 2406149.
(9) Liu, T.; Liu, T.; Gao, F.; Glotzer, S. C.; Solomon, M. J. Structural Color Spectral Response of Dense Structures of Discoidal Particles Generated by Evaporative Assembly. *J. Phys. Chem. B* **2022**, *126*, 1315−1324.
(10) Wang, J.; Le-The, H.; Shui, L.; Bomer, J. G.; Jin, M.; Zhou, G.; Mulvaney, P.; Pinkse, P. W. H.; van den Berg, A.; Segerink, L. I.; et al. Multilevel Spherical Photonic Crystals with Controllable Structures and Structure-Enhanced Functionalities. *Adv. Opt. Mater.* **2020**, *8* (10), 1902164.
(11) Areias, L. R. P.; Marcelo, G.; Farinha, J. P. S. Polymer Nanoparticle-Based Spherical Photonic Pigments for Dye-Free Noniridescent Bright Coloring. *ACS Appl. Nano Mater.* **2021**, *4*, 13185−13195.
(12) Mbah, C. F.; Wang, J.; Englisch, S.; Bommineni, P.; Varela-Rosales, N. R.; Spiecker, E.; Vogel, N.; Engel, M. Early-Stage Bifurcation of Crystallization in a Sphere. *Nat. Commun.* **2023**, *14* (1), 5299.
(13) Wu, X.; Hong, R.; Meng, J.; Cheng, R.; Zhu, Z.; Wu, G.; Li, Q.; Wang, C.; Chen, S. Hydrophobic Poly(tert-butyl acrylate) Photonic Crystals towards Robust Energy-Saving Performance. *Angew. Chem. Int. Ed.* **2019**, *58*, 13556−13564.
(14) Wang, H.; Cai, L.; Zhang, D.; Shang, L.; Zhao, Y. Responsive Janus Structural Color Hydrogel Micromotors for Label-Free Multiplex Assays. *Research* **2021**, *2021*, 9829068.
(15) Yang, S.; Kim, Y. G.; Park, S.; Kim, S. H. Structural Color Mixing in Microcapsules through Exclusive Crystallization of Binary and Ternary Colloids. *Adv. Mater.* **2023**, *35*, 2302750.
(16) Zhou, K.; Tian, T.; Wang, C.; Zhao, H.; Gao, N.; Yin, H.; Wang, P.; Ravoo, B. J.; Li, G. Multifunctional Integrated Compartment Systems for Incompatible Cascade Reactions Based on Onion-Like Photonic Spheres. *J. Am. Chem. Soc.* **2020**, *142*, 20605−20615.
(17) Lin, Z.; Gong, Z.; Bower, D. Q.; Lee, D.; Deravi, L. F. Bidispersed Colloidal Assemblies Containing Xanthommatin Produce Angle-Independent Photonic Structures. *Adv. Opt. Mater.* **2021**, *9* (24), 2100416.
(18) Kim, S. H.; Jeon, S. J.; Jeong, W. C.; Park, H. S.; Yang, S. M. Optofluidic Synthesis of Electroresponsive Photonic Janus Balls with Isotropic Structural Colors. *Adv. Mater.* **2008**, *20*, 4129−4134.
(19) Yu, Z.; Wang, C.; Ling, L.; Chen, L.; Chen, S. Triphase Microfluidic-Directed Self-Assembly: Anisotropic Colloidal Photonic Crystal Supraparticles and Multicolor Patterns Made Easy. *Angew. Chem. Int. Ed.* **2012**, *51*, 2375−2378.
(20) Lee, G. H.; Jeon, T. Y.; Kim, J. B.; Lee, B.; Lee, C. S.; Lee, S. Y.; Kim, S. H. Multicompartment Photonic Microcylinders toward Structural Color Inks. *Chem. Mater.* **2018**, *30*, 3789−3797.
(21) He, Q.; Ku, K. H.; Vijayamohanan, H.; Kim, B. J.; Swager, T. M. Switchable Full-Color Reflective Photonic Ellipsoidal Particles. *J. Am. Chem. Soc.* **2020**, *142*, 10424−10430.
(22) Zhao, Y.; Xie, Z.; Gu, H.; Jin, L.; Zhao, X.; Wang, B.; Gu, Z. Multifunctional Photonic Crystal Barcodes from Microfluidics. *NPG Asia Mater.* **2012**, *4*, No. e25.
(23) Jana, S.; Um, S. H.; Jung, S. Paramecium Swimming in Capillary Tube. *Fluids* **2012**, *24* (4), 041901.
(24) Sim, J. Y.; Lee, G. H.; Kim, S. H. Microfluidic Design of Magnetoresponsive Photonic Microcylinders with Multicompartments. *Small* **2015**, *11*, 4938−4945.
(25) Lee, H. S.; Kim, J. H.; Lee, J. S.; Sim, J. Y.; Seo, J. Y.; Oh, Y. K.; Yang, S. M.; Kim, S. H. Magnetoresponsive Discoidal Photonic Crystals Toward Active Color Pigments. *Adv. Mater.* **2014**, *26*, 5801−5807.
(26) Li, P.; Pang, H.; Zheng, Y.; Cui, Q.; Shang, C.; Xiao, Y.; Hui, T.; Hu, Y. Composite Photonic Microobjects with Anisotropic Photonic Properties from a Controlled Wet Etching Approach. *Colloids Surf., A* **2024**, *688*, 133618.
(27) Fang, Z.; Keinan, S.; Alibabaei, L.; Luo, H.; Ito, A.; Meyer, T. J. Controlled Electropolymerization of Ruthenium(II) Vinylbipyridyl Complexes in Mesoporous Nanoparticle Films of TiO_2. *Angew. Chem. Int. Ed.* **2014**, *53*, 4872−4876.
(28) Stöber, W.; Fink, A.; Bohn, E. Controlled Growth of Monodisperse Silica Spheres in the Micron Size Range. *J. Colloid Interface Sci.* **1968**, *26*, 62−69.
(29) Cheng, Y.; Zhu, C.; Xie, Z.; Gu, H.; Tian, T.; Zhao, Y.; Gu, Z. Anisotropic Colloidal Crystal Particles from Microfluidics. *J. Colloid Interface Sci.* **2014**, *421*, 64−70.
(30) Shang, L.; Xu, K.; Lu, P. J.; Abbaspourrad, A.; Zhao, Y.; Weitz, D. A. Dramatic Droplet Deformation through Interfacial Particles Jamming. *Proc. Natl. Acad. Sci. U. S. A.* **2024**, *121* (42), No. e2403953121.
(31) Cai, Q.; Ju, X.; Chen, C.; Faraj, Y.; Jia, Z.; Hu, J.; Xie, R.; Wang, W.; Liu, Z.; Chu, L. Fabrication and Flow Characteristics of Monodisperse Bullet-Shaped Microparticles with Controllable Structures. *Chem. Eng. J.* **2019**, *370*, 925−937.
(32) Liu, X.; Liu, J.; Wei, B.; Yang, D.; Luo, L.; Ma, D.; Huang, S. Bio-Inspired Highly Brilliant Structural Colors and Derived Photonic Superstructures for Information Encryption and Fluorescence Enhancement. *Adv. Sci.* **2023**, *10* (24), 2302240.
(33) Wu, Y.; Wang, Y.; Zhang, S.; Wu, S. Artificial Chameleon Skin with Super-Sensitive Thermal and Mechanochromic Response. *ACS Nano* **2021**, *15*, 15720−15729.
(34) Kim, J. B.; Kim, J. W.; Kim, M.; Kim, S. H. Dual-Colored Janus Microspheres with Photonic and Plasmonic Faces. *Small* **2022**, *18* (21), 2201437.
(35) Michaudel, Q.; Kottisch, V.; Fors, B. P. Cationic Polymerization: From Photoinitiation to Photocontrol. *Angew. Chem. Int. Ed.* **2017**, *56*, 9670−9679.

https://doi.org/10.1021/acsami.4c20550
ACS Appl. Mater. Interfaces 2025, 17, 15969−15977